Simulation of CHF Condition using an Electroplating System

Seung-Min Ohk, Hae-Kyun Park, Bum-Jin Chung*
Department of Nuclear Engineering, Kyung Hee University
#1732 Deogyeong-daero, Giheung-gu, Yongin-si, Gyeonggi-do, 17104, Korea
**Corresponding author: bjchung@khu.ac.kr*

1. Introduction

Heat transfer is enhanced when the bubbles are generated on the heated surface at the nucleate boiling regime since vigorous mixing of the liquid occurs near the heated surface due to the buoyancy force of the bubbles. However, as this phenomenon intensified, vapor film can be formed on the heated surface and it impairs heat transfer disturbing the heat exchange between the surface and the bulk liquid. And thus, the heat flux has the certain maximum value [1]. This maximum value, Critical Heat Flux (CHF) is generally exhibits in the pool boiling condition in non-film boiling mode. Actually, the higher heat flux could be generated at the film boiling mode with extremely high surface temperature, which may unendurable for the system structure. Therefore, CHF is the crucial parameter in the design criterion at the heat exchanger system in human industry [2, 3]. Especially for the nuclear power plant, the integrity of the heat exchange system have been treated with great care in respect of the CHF: peak power of the reactor is governed by the CHF value in the fuel assembly and the integrity of the reactor vessel could be determined by the CHF value when a severe accident is occurs.

Mechanism of the CHF have been studied for several decades [4-11]. However, this is not clarified so far and it is hard to simulate CHF situation due to the high superheat is needed. This study proposes the non-heating experimental method to simulate CHF situation using mass transfer electroplating system. It is much easier to generate gas over the surface via reduction reaction of the hydrogen ions. $CuSO_4$–H_2SO_4 as the electrolyte, copper plate is used for both anode and cathode for electroplating system.

2. Existing studies

Various researchers have been studied for CHF phenomena of pool boiling conditions experimentally and analytically. Although a number of CHF models have been postulated and proposed for last half a century, however, the physical mechanism has not been determined precisely [4].

2.1 Hydrodynamic Instability Model

Zuber [5] established hydrodynamic instability model, which have been widely accepted. In an earlier study, Kutateladze [6] proposed CHF predicted correlation based on a dimensional analysis. Zuber developed Kutateladze correlation applying to the Rayleigh-Taylor instability. Heated surface and vapor column are presented through the Rayleigh-Taylor instability. In this case, vapor column diameter assumed a half of Rayleigh-Taylor wavelength. At CHF condition, vapor velocity assumed by Kelvin-Helmholtz instability. Compared with the existing experimental data, *K* value would be 0.131.

$$q''_{CHF} = K h_{lg} \rho_g^{1/2} [\sigma g(\rho_l - \rho_g)]^{1/4} \quad (1)$$

2.2 Macrolayer Dryout Model

Haramura and Katto [7] proposed the macrolayer dryout model. They improved Katto and Yokoya's study [8] and insisted that heat transfer at high heat flux is related with presence of macrolayer. Macrolayer is located upon the heater and underneath of the vapor mushroom. It is composed of vapor stems and liquid. The thickness of macrolayer is postulated by Haramura and Katto as a forth of Kelvin-Helmholtz wavelength. CHF occurs when liquid in macrolayer is completely vaporized during hovering time, which is a period from generation to departure of the vapor mushroom. They proposed CHF predicted correlation from the heat balance equation, which is derived in terms of the liquid vaporization in the macrolayer.

$$\tau_d q''_{CHF} = \delta_l h_{lg} \rho_l (A_h - A_v) \quad (2)$$

τ_d, δ_l, A_h and A_v is hovering period, thickness of macrolayer, heated area, and area of vapor stem respectively. Eq. (2) can be present that following Eq. (3)

$$q''_{CHF} = h_{lg} \rho_g^{0.5} [\sigma g(\rho_l - \rho_g)]^{1/4} (1+k)^{5/16} \left(\frac{\pi^4}{2^{11} \cdot 3^2}\right)^{1/16} \quad (3)$$
$$\left(\frac{A_v}{A_w}\right)^{5/8} \left(1 - \frac{A_v}{A_w}\right)^{5/16} \left[\left(\frac{\rho_l}{\rho_g} + 1\right) / \left(\frac{11}{16}\frac{\rho_l}{\rho_g} + 1\right)^{3/5}\right]^{5/16}.$$

2.3 Other Models

Besides those correlations, Kandlikar [9] interpreted the CHF theoretically in terms of vapor bubble receding contact angle. It means that receding contact angle between surface and bubble may effect of the CHF. He suggested CHF correlation, which is well agreed with

Kutateladze's correlation and existing test results. However, Kandlikar's model predicted well rather than Kutateladze's model for the vertical plates. Because the suggested correlation considered both hydrodynamic effect and non-hydrodynamic effect such as bubble receding contact angle and orientation of the surface.

Also as high speed camera recording technology advanced, many researchers can be observed and analyzed CHF phenomena in detail [10-12]. Ahn and Kim [12] shows presence of macrolayer and dry patch at the vicinity of CHF using high speed camera. For a small heater, CHF is increased due to inflow effect at the edge of the heater. Because the inflow liquid interrupted vaporization. For the same reason, macrolayer forms as concave shape.

3. Experiments

3.1 Methodology

The copper sulfate–sulfuric acid ($CuSO_4$–H_2SO_4) electroplating system was adopted to simulate CHF phenomenon. The system is composed of anode and cathode electrodes submerged in a solution of copper sulfate and sulfuric acid. As the applied potential between anode and cathode increases, the current increases initially and then reaches a plateau, where a further increase in the applied potential does not affect the current. In this case, the current at the plateau is termed the limiting current (Figure 1: Limiting current curve).

At a higher potential beyond the limiting current region, hydrogen ions reduces and the current increases, resulting in the evolution of hydrogen gas. This phenomenon is similar to the vapor production in the heat transfer system.

The basic idea of this study is that the CHF phenomenon due to the departure of nucleate boiling and film formation by the generation of vapor can be simulated by the hydrogen gas generation in an electroplating system. If hydrogen gas generation exceeds a certain limit, hydrogen film can be made. Although it is strictly differ from the two-phase flow to the two-component flow in terms of the chemical identity, there are several points of similarity between them: general phenomenon, analysis and experimental method [13].

In the two phase flow, hydraulic behaviors of gas over the corresponding solid surface will be similar under identical gaseous volume condition, when several physical properties of the fluid are defined. Thus, fundamental relation between heat flux and mass flux, which resulted in the same volume generation rate of vapor and hydrogen gas were defined as follow:

$$\eta = \frac{I}{n \times e \times N_A} \tag{4}$$

Gas generation rate (Mole/s), η can be calculated by the applied current, I of the electroplating system over products between n, e and N_a, which represent number of the electron charge to reduction hydrogen ion, magnitude of the charge of an electron and Avogadro constant, respectively. And the applied heat flux is simulated as follows

$$q = \eta \times h_{fg} \times M_{a,vapor} \tag{5}$$

Hydrogen gas generation rate, as calculated in the electroplating system in Eq. (4) substitutes vapor generation term, η of Eq. (5) with an isovolumetric concept. Then, the product of latent heat, h_{fg} and atomic number of the vapor $M_{a,vapor}$ transforms the applied current in the electroplating system into the heat flux in the heat transfer system.

3.2 Experimental Apparatus

The experimental apparatus and diagram are shown in Fig. 1. A horizontal upward facing copper plate is located in a top-opened acrylic tank. This cathode plate of 0.01 m × 0.01 m simulates heated surface. And a anode copper plate of 0.1 m × 0.2 m is placed against the cathode to supply electric charges. The power supply (SGI 100A/150V, SGI) was used for current control and Data Acquisition system (34972A, Agilent) was used for recording the data.

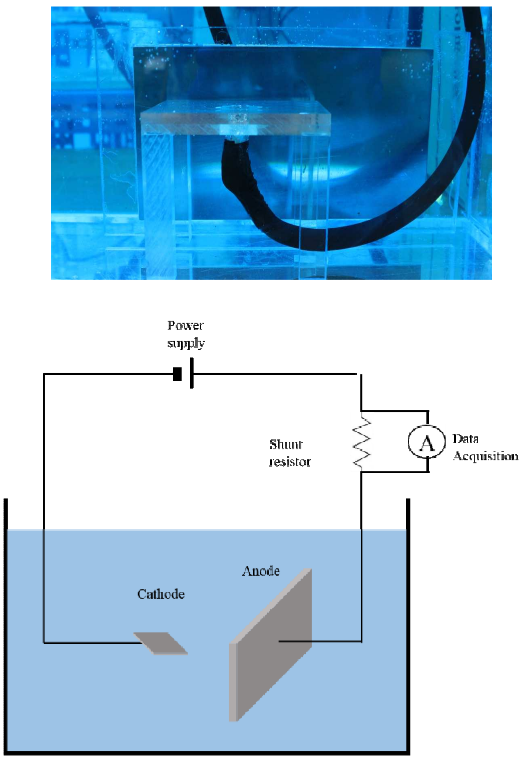

Fig. 1. Photograph of the test apparatus and electric circuit.

4. Results and discussion

4.1 Similarity

Figure 2 shows the measured current (*I*) and potential (*V*) during experiment. Potential increased as applied current increased at low-current region, which is similar with nucleate boiling region of the boiling curve. When current density reaches about 270 kA/m^2, potential increased immediately, while current density decreased. It seems that the coalescence of bubble (mushroom) on the cathode plate blocked supplement of the electron charge. So that the potential increased greatly as the resistance increased.

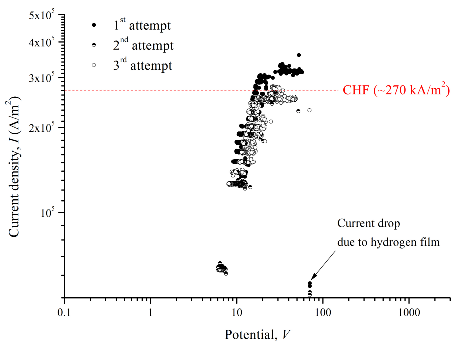

Fig. 2. CHF simulation result using electroplating system.

Figure 3 compares the hydrogen bubble and vapor behavior with respect to the bubble growth to the CHF situation. When the low current density, discrete bubble generated and departed from the surface. As applied current density increased, large bubble appeared due to increased bubble interaction as nucleate boiling site and bubble departure frequency increased. Those bubble behavior are similar to those on heat transfer system as shown in Fig. 3.

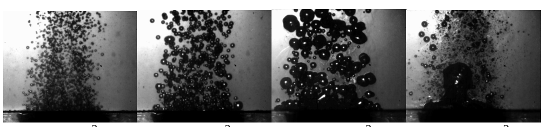

(a)Hydrogen bubble in mass transfer.

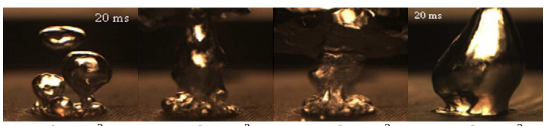

(b) Vapor bubble in heat transfer [12].

Fig. 3. Bubble behavior similarity.

4.1 Comparison with Heat Transfer Results and Parametric Analysis

The CHF was simulated by electroplating system at the current density of 270 kA/m^2. Thus, using Eq. (5), applied heat flux is calculated as 56.8 kW/m^2. However, the CHF triggers in heat transfer system, when heat flux is over 1000 kW/m^2 for saturated water in atmospheric pressure.

Table 1. Physical parameters of two different systems.

	Heat transfer (Sat. Water)	Mass transfer ($CuSO_4$–H_2SO_4 solution)
CHF (kW/m^2)	1,105.2	56.8 (Simulated)
Bulk temperature (°C)	100	60
Liquid density (kg/m^3)	957	983 (Water)
Vapor density (kg/m^3)	0.596	0.073 (Hydrogen)
Surface tension (N/m)	0.059	0.062 (Water)
Gas generation	$H_2O(g) \leftrightarrow H_2O(l)$	$2H_3O^+ + 2e^- \rightarrow H_2 + 2H_2O$
Reaction formula	Two phase	Two component

Table 1 listed the physical parameters and major differences between water and $CuSO_4$–H_2SO_4 solution. Zuber interpreted vapor column arrangement and collapse using hydrodynamic instabilities. Induced correlation is combined with parameters of vapor and liquid density, gravity, and surface tension. So that we considered main parameters of Zuber's CHF predicted correlation. We assume that CHF occurred when the same volume of vapor of hydrogen. Thus we used vapor density term ($\rho_g^{1/2}$) from hydrogen gas to vapor. Also $[\sigma g(\rho_l\text{-}\rho_g)]^{1/4}$ term is considered. But there is a little difference in value, since σ and $\rho_l\text{-}\rho_g$ are similar between water and $CuSO_4$–H_2SO_4 solution as listed in Table 1. Finally, the value of CHF in Eq. (5) is revised by the ρ_g difference, from 56.8 kW/m^2 to 167.26 kW/m^2. However, CHF with horizontal upward facing heater for saturated water at atmospheric pressure is predicted 1105.2 kW/m^2 according to Zuber correlation and similar scale was measured in other researchers. The discrepancy with this study will be investigated in further works.

5. Conclusion

CHF phenomena is simulated by hydrogen gas using electroplating system in mass transfer experiment. Vapor behavior on mass transfer experiment was visualized, and it was similar to that of on the heat transfer.

CHF value was simulated by hydrogen gas with isovolumetric concept. Thus, virtual heat flux was estimated by mass flux, which is a non-heating process. Difference of gas density from heat transfer and mass transfer systems were considered and revised for the simulated heat flux. Despite of the simple parametric analysis, estimated CHF value of this study was 6.6 times smaller than Zuber's.

Consequently, consideration for this discrepancy needs additional parametric analysis: two phase and two component system, surface wettability, copper reduction phenomenon on the surface, etc.

ACKNOWLEDGMENT

This study was sponsored by the Ministry of Science, ICT and Future Planning (MSIP) and was supported by Nuclear Research and Development program grant funded by the National Research Foundation (NRF) (Grant Code: 2014M2A8A1030777).

REFERENCES

[1] F. P. Incropera, Foundation of Heat Transfer, John Wiley & Sons, New Yotk, pp. 622-638, 2012.
[2] N. E. Toderas, M. S. Kazimi, Nuclear systems, CRC press, New York, pp. 697-819, 2011.
[3] Z. Zhao, S. Glod, D. Poulikakos, Pressure and power generation during explosive vaporization on a thin-film microheater, International Journal of Heat and Mass Transfer, Vol.43, pp. 281-296, 2000.
[4] P. Sadasivan, P. R. Chappidi, C. Unal, R. A. Nelson, Possible mechanisms of macrolayer formation, International Communication in Heat and Mass Transfer, Vol.19, pp. 801-815, 1992.
[5] N. Zuber, Hydrodynamic aspects of boiling heat transfer, AEC Report No. AECU-4439, Physics and Mathematics, 1959.
[6] S. S. Kutateladze, A hydrodynamic model of the critical heat transfer in boiling liquids with free convection, Zhurn. Tekhc., Fiz., Vol.20, pp. 1389-1392, 1950.
[7] Y. Haramura and Y. Katto, A new hydrodynamic model of critical heat flux, applicable widely to both pool and forced convective boiling on submerged bodies in saturated liquids, International Journal of Heat and Mass Transfer, Vol.26, pp. 389-399, 1983.
[8] Y. Katto and S. Yokoya, Principal mechanism of boiling crisis in pool boiling, International Journal of Heat and Mass Transfer, Vol.11, pp. 993-1002, 1968.
[9] S. G. Kandlikar, A theoretical model to predict pool boiling CHF incorporating effects of contact angle and orientation, Journal of Heat Transfer, Vol.123, pp. 1071-1079, 2001.
[10] H. J. Van Ouwerkerk, Burnout in pool boiling the stability of boiling mechanisms, International Journal of Heat and Mass Transfer, Vol. 15, pp. 25-34, 1972.
[11] I. C. Bang, S. H. Chang, W. P. Beak, Visualization of a principle mechanism of critical heat flux in pool boiling, International Journal of Heat and Mass Trasnfer, Vol.48, pp. 5371-5385, 2005.
[12] H. S. Ahn, M. H. Kim, Visualization study of critical heat flux mechanism on a small and horizontal copper heater, International Journal of Multiphase Flow, Vol.41, pp. 1-12, 2012.
[13] G. B. Wallis, One-dimensional two-phase flow, McGraw-Hill, 1969.